Sensors and Actuators B 185 (2013) 195–200

Contents lists available at SciVerse ScienceDirect

Sensors and Actuators B: Chemical

journal homepage: www.elsevier.com/locate/snb

Evanescently coupled mid-infrared photodetector for integrated sensing applications: Theory and design

Vivek Singh[a,*], Timothy Zens[a,b], Juejun Hu[c], Jianfei Wang[a], J. David Musgraves[d], Kathleen Richardson[d], Lionel C. Kimerling[a], Anu Agarwal[a]

[a] Microphotonics Center, Massachusetts Institute of Technology, Cambridge, MA 02139, United States
[b] Department of Engineering Physics, Air Force Institute of Technology, Wright-Patterson AFB, OH 45433, United States
[c] Department of Materials Science and Engineering, University of Delaware, Newark, DE 19716, United States
[d] School of Materials Science and Engineering, Clemson University, Clemson, SC 29634, United States

ARTICLE INFO

Article history:
Received 21 December 2012
Received in revised form 14 April 2013
Accepted 16 April 2013
Available online xxx

Keywords:
Infrared
Photoconductivity
Photodetectors
Glass waveguides
Lab-on-a-chip

ABSTRACT

We present theory and simulation of a mid-infrared ($\lambda = 3.2\,\mu m$) chalcogenide waveguide monolithically integrated with an evanescently coupled PbTe photodetector for lab-on-a-chip sensing applications. A spacer layer is used to modify effective index of the structure, enabling a waveguide-detector mode to propagate in the chalcogenide waveguide and be absorbed in the PbTe detector. The relation between quantum efficiency and detector dimensions is analyzed showing that the design geometry can be optimized to maximize signal to noise ratio. In addition, the location of metal contacts is optimized to minimize loss while maintaining good device performance. The design is compatible with standard planar lithographic processing and its flexibility suggests multiple applications in the fields of biological and chemical sensing.

1. Introduction

IR spectroscopy for the identification of biological and chemical agents is usually performed in the "fingerprint" midwave-infrared (MWIR) bands from 3 to 5 μm and 8 to 12 μm where most molecules show characteristic vibrational absorption features. Rapid sensing and detection with high sensitivity in a small footprint can be achieved by the integration of various functional elements (mid-IR light source, sensing element, detector, and read-out circuits) onto a monolithic, planar silicon platform as schematically illustrated in Fig. 1. Smaller device footprints can lead to new and important applications such as remote deployment of arrays of integrated mid-IR sensor devices that can record and relay data from sensing events without human intervention.

Although there have been successful demonstrations of mid- and far-IR transmission and sensing with III–V waveguides (GaAs/AlGaAs) [1,2] and silver halides (AgBr/AgCl) [3], they remain low-index contrast systems with high cost (III–V systems grown using MOCVD/MBE) or feature high sidewall roughness (silver halide) in single-mode designs. Chalcogenide glasses (ChGs) have recently been demonstrated as a promising platform for mid-IR chemical and biological sensing [4] since they exhibit transparency over a large range of mid-IR wavelengths and tunable optical properties through doping and/or compositional tailoring [5]. A CMOS-backend-compatible process can be employed to fabricate ChG-based planar devices on a silicon platform [6], reducing the cost and footprint when compared to traditional chemical and biological sensors.

Broadband infrared (IR) detectors such as those based on HgCdTe have been extensively used in IR spectroscopy [7] – they are typically single-crystalline and are obtained by high-cost growth techniques such as metal organic chemical vapor deposition (MOCVD) and molecular beam epitaxy (MBE) [8]. We have recently demonstrated a thin film lead telluride (PbTe) photoconductor as an efficient on-chip IR detector of choice due to: (a) the ease of deposition of single-phase, stoichiometric polycrystalline PbTe films using low cost thermal evaporation techniques and (b) for its superior chemical stability [9,10]. Also, a resonant-cavity-enhanced dual band mid-IR detector has recently been demonstrated using PbTe as the active absorber [11].

Our integrated sensor approach uses vertical evanescent coupling from ChG waveguides (As_2Se_3) into MWIR PbTe detectors. An inherent challenge is the large index difference at $\lambda = 3.2\,\mu m$ between As_2Se_3 ($n = 2.75$) and PbTe ($n = 5.2$) which is addressed by the introduction of a low index spacer layer between the waveguide and detector to minimize modal mismatch and Fresnel

* Corresponding author. Tel.: +1 6172533157.
E-mail address: vsingh@mit.edu (V. Singh).

0925-4005/$ – see front matter © 2013 Elsevier B.V. All rights reserved.
http://dx.doi.org/10.1016/j.snb.2013.04.065

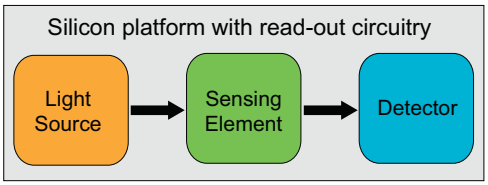

Fig. 1. Schematic illustration of an integrated sensor device that combines a light source, sensing elements, a detector, and read-out circuitry on a monolithic silicon platform.

reflection. Evanescently coupled detectors using hybrid integration of III–V detectors for 2.2–2.3 μm detection [12] and monolithically integrated Ge detectors for telecom wavelengths have been demonstrated [13]. However, we present here a design and simulation results for a new and important wavelength range useful in chem-bio sensing. We demonstrate a mid-IR waveguide-detector integration scheme using a ChG waveguide monolithically integrated with an MWIR PbTe photoconductive detector. Unlike their bulky off-chip counterparts, mid-IR microsensor arrays integrated with PbTe detectors can enable the *low-cost*, *small footprint*, *remote* detection of multiple chemical/biological species on a single silicon platform.

2. Materials and methods

2.1. Design

Fig. 2(a) shows the layout of the evanescently coupled detector and Fig. 2(b) shows a cross section of the detector waveguide

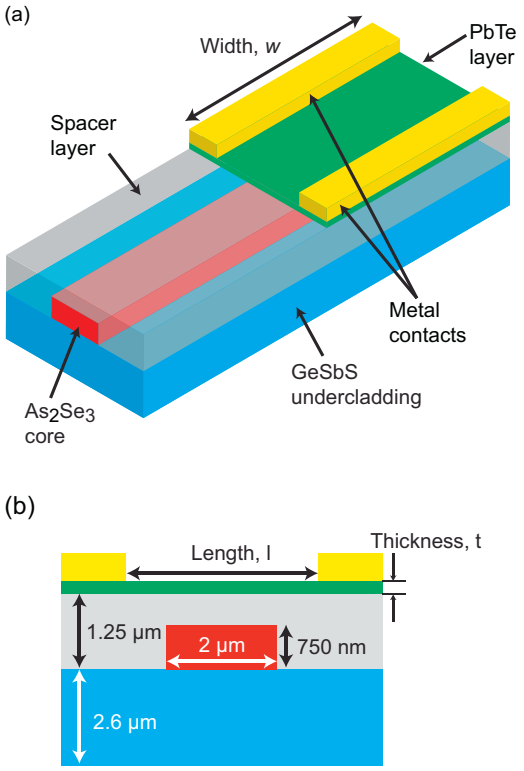

Fig. 2. (a) Integrated structure with a single mode (λ = 3.2 μm) As_2Se_3 waveguide, GeSbS glass undercladding to prevent leakage of mode into Si substrate, low index spacer to minimize modal mismatch and Fresnel reflection, and the photoconductive PbTe layer. (b) Cross section of the device with dimensions used for design and simulation.

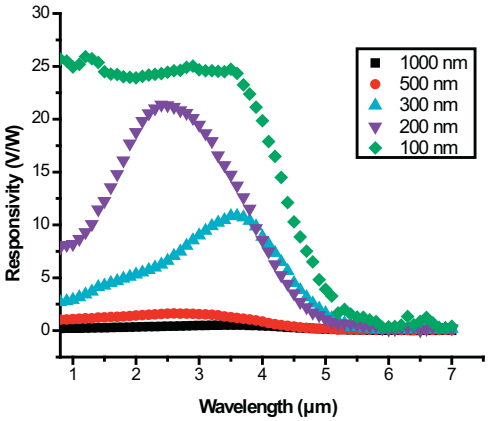

Fig. 3. Responsivity of polycrystalline PbTe films of different thicknesses under a bias current of 0.1 mA and cooled to −60 °C by a thermoelectric cooler (TEC). While all films show good photoconductive signal, the 100 nm film exhibits the highest responsivity.

system. The As_2Se_3 waveguide is designed for single mode operation at 3.2 μm and the GeSbS glass ($n = 2.1$) undercladding prevents leakage into the silicon substrate. The spacer (nominally $n = 1.5$) in Fig. 2(a) covers the entire sample and also functions as a planarizing layer, with the PbTe extending laterally beyond the waveguide.

Prior work has studied the responsivity of thermally evaporated polycrystalline PbTe thin films. The photoresponsivity of polycrystalline PbTe was optimized by measuring thin films of different thicknesses both, at room temperature and at thermoelectrically cooled temperatures (−60 °C or 214 K). The 100 nm thick PbTe detector layer exhibits high photoresponsivity (25 V/W) in the 3–4 μm wavelength range under a bias current of 0.1 mA at −60 °C as shown in Fig. 3 [10,14,15]. From a materials perspective, further improving the responsivity of polycrystalline PbTe films for mid-IR detection may be possible by increasing carrier lifetime or by reducing carrier concentration. For example, incorporation of oxygen in lead chalcogenide films can enhance carrier lifetimes due to spatial separation of photo-generated electrons and holes by minority carrier traps (PbO^+) [16–19]. The oxygen also forms acceptor states in the band gap which deplete electrons from the conduction band. Oxygen sensitization is typically achieved using high temperature (>450 °C) anneals in an oxidizing atmosphere [20,21] and for the monolithically integrated structure that we are proposing, such anneals for the PbTe layer will have detrimental effects on the ChG materials underneath. However, we have demonstrated that room temperature oxygen sensitization of PbTe is possible and leads to improved responsivity [14,15]. In this paper, we will focus on improving waveguide-detector coupling performance by optimizing the geometry of the PbTe detector layer for a high signal-to-noise ratio.

2.2. Detector theory

Detector optimization requires that we examine the physics underpinning the signal to noise ratio. The change in voltage in the illuminated portion of the photoconductor with an applied current bias is given by:

$$\Delta V = I \times \Delta R = I \times \left[\frac{1}{\sigma + \Delta\sigma} - \frac{1}{\sigma}\right] \frac{l}{wt} \approx I \frac{l}{wt} \times \frac{-\Delta\sigma}{\sigma^2}, \Delta\sigma << \sigma \quad (1)$$

where w and t are the width and the thickness of the photoconductor, l is the length parallel to the bias current I, ΔR is the change in

resistance, σ is the conductivity, and we assume that PbTe exhibits long carrier lifetimes. The change in conductivity ($\Delta\sigma$) is related to changes in carrier concentration and to changes in mobility [22]:

$$\sigma = ne\mu_n + pe\mu_p \rightarrow \Delta\sigma = (\Delta ne\mu_n + \Delta pe\mu_p) + (ne\Delta\mu_n + pe\Delta\mu_p) \quad (2)$$

where n and p are the electron and hole concentrations, e is the elementary charge, and μ_n and μ_p are the electron and hole mobilities. The change in conductivity can thus be written as the sum of the changes due to carrier concentration (first term) and the mobility (second term):

$$\Delta\sigma = (\Delta\sigma)_{cc} + (\Delta\sigma)_{\mu} \quad (3)$$

Our PbTe photoconductive films show no change in mobility with illumination therefore the barrier modulation contribution [23] linked to the change in mobility may be ignored and we adopt number modulation theory [24], which has produced results consistent with experimental measurements on our previous photodetector devices [15]. As the lifetimes of electrons and holes in our materials are nearly equal we can equate Δn and Δp, to express the change in the number of carriers as:

$$\Delta n = \Delta p = \frac{\tau}{(hc/\lambda)ltw^2}\int_0^w P(w)dw \rightarrow \frac{\eta\tau P_{opt}}{(hc/\lambda)ltw} \quad (4)$$

where P_{opt} is total optical power sent down the waveguide (integrated over the width w), λ is the wavelength of illumination, τ is the photo-generated carrier lifetime, η is the quantum efficiency, h is Planck's constant and c is the velocity of light. We can assume that incident optical power is distributed evenly along the propagation direction of the waveguide, and thus we can combine Eq. (2) and Eq. (4):

$$\Delta\sigma = \frac{e\eta\lambda\tau(\mu_n + \mu_p)P_{opt}}{hc \times lwt} \quad (5)$$

Defining the responsivity $\Re$ as the change in voltage over the incident light power (V/W) and setting $\sigma = pe\mu_p$ for a p-type system we can combine Eq. (1) and Eq. (5) to get

$$\Re = \frac{I\eta\lambda\tau(1+b)}{hce \times w^2t^2p^2\mu_p} \rightarrow \Re \propto \frac{\eta}{(wt)^2} \quad (6)$$

where b is the electron-hole mobility ratio and w and t are the width and the thickness of photoconductor. To optimize the design we focus on the dimensions of the photoconductor, thus simplifying the equation. For photoconductive detectors, shot noise is non-existent and at reasonably high chopping frequencies, Johnson noise, defined as $V_J = [4kTR_d\Delta f]^{1/2}$, is the dominant noise contributor in our detectors [15,25] where R_d is the dark space resistance of the entire detector and Δf is the bandwidth. We use a noise voltage because we hold current constant and measure a change in the voltage. If we assume that $\Delta\sigma \ll \sigma$, the signal-to-noise ratio (SNR) becomes:

$$\text{SNR} \propto \sqrt{\frac{\eta^2}{w^3t^3l}} \quad (7)$$

From Eq. (7) we see that thinner and shorter detectors maximize the SNR, but our simulations show that the quantum efficiency is also linked to detector dimensions.

2.3. Integrated detector simulations

For the structure shown in Fig. 2, the modes were first calculated using the commercially available mode solver FIMMWAVE and then injected into FIMMPROP (both by Photon Design) to study the field distribution during propagation. In addition to simulating mode behavior in the integrated structure, detailed 3D finite-difference time-domain (FDTD) simulations were also carried out with Lumerical's FDTD Solutions package to find optimal values of the detector dimensions that lead to the highest quantum efficiency. A conformal mesh size setting of 6 was used for the entire structure with a finer mesh (10 nm) chosen for the PbTe layer due to the lower thickness. The light source in Lumerical was a single wavelength mode source at $\lambda = 3.2$ μm. Note that we will refer to the internal quantum efficiency of the detector as the quantum efficiency for this analysis and assume that lifetimes and current applied are held constant as we change dimensions.

3. Results and discussion

Fig. 4 illustrates the role of the spacer layer; Fig. 4(a) shows the field distribution with the PbTe placed directly on top of the waveguide while Fig. 4(b) demonstrates the effect of adding the spacer layer shown in Fig. 2. Without a spacer layer, the incident power is concentrated in the first 10 μm and such a design is undesirable due to high Fresnel reflection arising from the large refractive index contrast between the waveguide and detector. The addition of the spacer layer helps to extend the distance over which the field is distributed as it modifies the effective index such that the waveguide-detector mode survives longer and the field distribution is more uniform. Fig. 4(c) shows the cross-sectional profile of the waveguide-detector mode.

Fig. 5 shows the effect of varying the width and thickness of the detector on the quantum efficiency. As the width of the photoconductor is increased, more light couples into the system increasing the quantum efficiency. However, the thickness of the detector

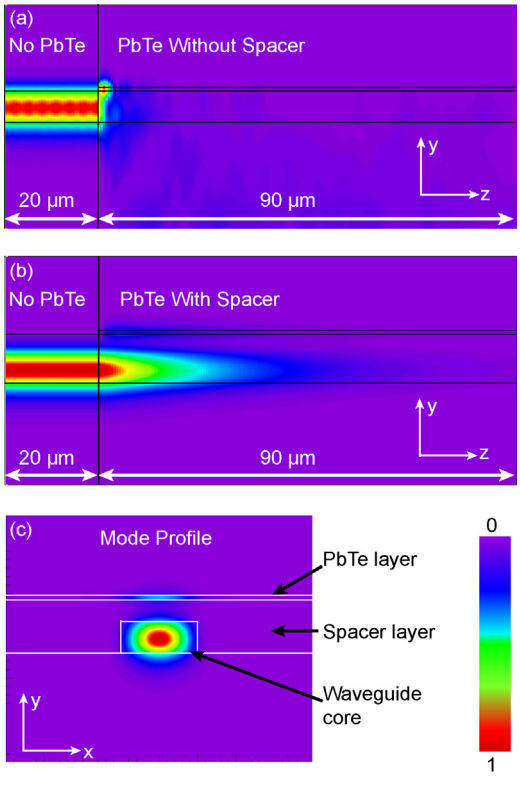

Fig. 4. (a) Cross section of field profile of evanescent detector without spacer layer shows that the mode is absorbed in the first 10 μm of the material. (b) Cross-sectional view of detector with spacer layer shows a less abrupt transition to the detector over 50–100 μm of detector width allowing for lower current densities. (c) Profile of the waveguide-detector mode with the field in both the waveguide and the PbTe layer.

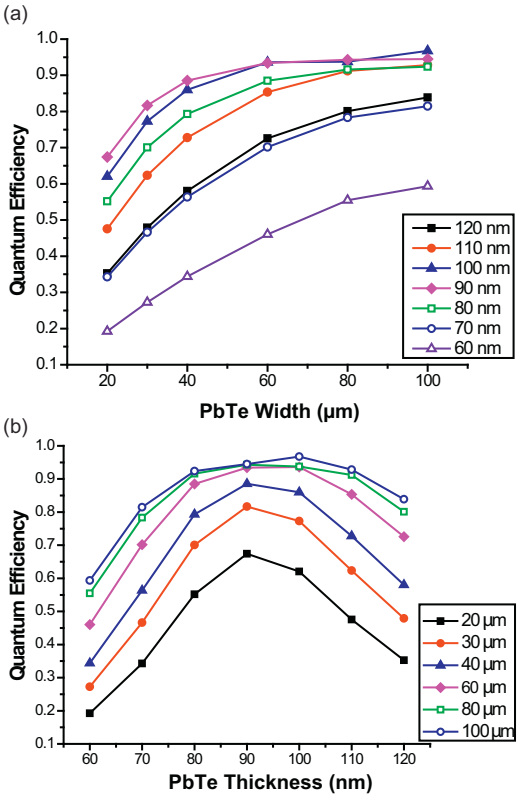

Fig. 5. (a) The relation between quantum efficiency and the detector width at various detector thicknesses shows higher quantum efficiency with increasing detector width as more light couples into the system. (b) The relation between quantum efficiency and the detector thickness at various detector widths shows that increasing the detector thickness increases the quantum efficiency as more of the propagating mode is contained in the detector. However, increasing the thickness beyond 90–100 nm alters the effective index to an extent that negatively impacts performance.

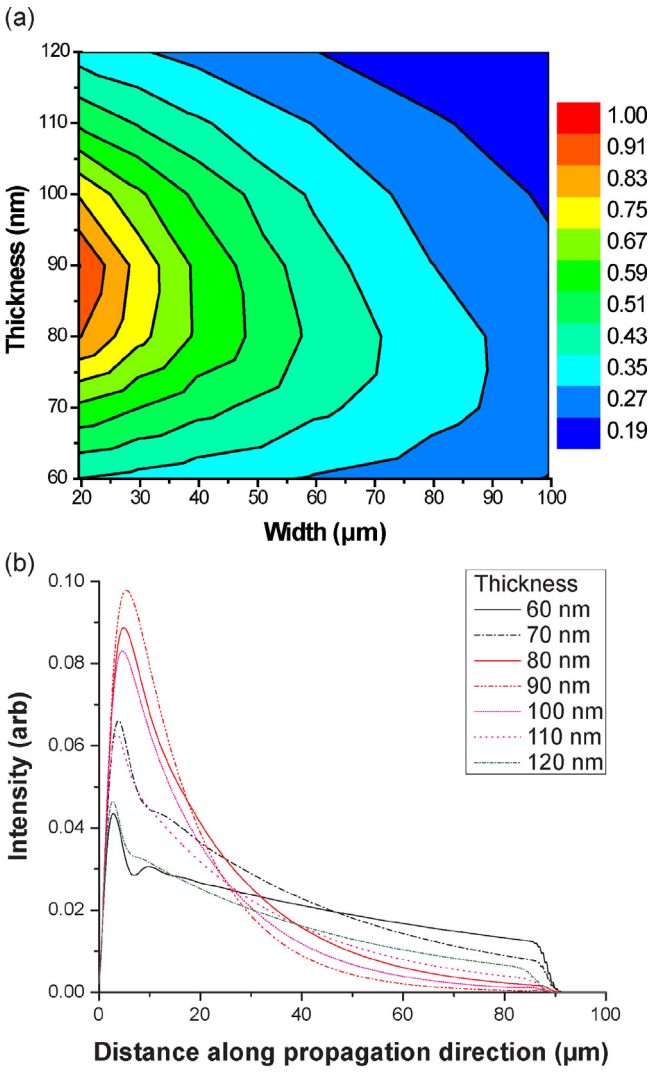

Fig. 6. (a) The effect of the width and thickness of the detector on the SNR figure-of-merit represented in a contour plot. (b) Intensity of the coupled light along the width of the detector.

sets the maximum quantum efficiency of the system which can be clearly seen in Fig. 5(b) where the quantum efficiency increases as the thickness of the detector increases up to 90–100 nm of thickness. A thicker film contains more of the evanescently coupled mode, thus increasing the likelihood of absorption. As films grow thicker than 100 nm the quantum efficiency decreases due to higher reflection resulting from the larger refractive index of PbTe. If the detector layer is too thin, an insufficient amount of light is absorbed which leads to lower quantum efficiency. Since a 100 nm thick film of PbTe was also demonstrated to exhibit the highest responsivity [15], 90–100 nm is chosen as the ideal thickness for our design.

These results can be inserted into Eq. (7) to evaluate the impact of the width and thickness on the device's SNR. Fig. 6(a) shows the normalized figure-of-merit (FoM) for the SNR of the detector – smaller widths are preferable even though the quantum efficiency is reduced due to the relatively small effect of detector width on quantum efficiency and the $w^{-3/2}$ dependence of SNR on width. In Fig. 6(b) we see that the intensity of the incident light is not constant; however, if we assume that charge carriers have sufficient mobility to drift toward areas of lower concentration and that even in the highest intensity areas the $\Delta\sigma \ll \sigma$ assumption still holds true, we do not have to alter the SNR FoM.

The length of the detector (distance between electrical contacts) also affects the SNR. Eq. (7) states that a shorter detector will improve the SNR but parasitic absorption losses from metal contacts can negatively impact the quantum efficiency. From FDTD simulations we have found that a minimum separation of 750 nm between the waveguide edges and the metal contacts is required to limit the change in quantum efficiency to less than 5%. Given the geometry shown in Fig. 2(b) this pins the minimum length of our devices to about 4 μm.

The choice of an appropriate spacer layer material is contingent on it meeting the primary requirements of transparency in the wavelength range of interest and relatively low refractive index. Ease of deposition should also be a consideration so that integrity of the lower waveguide layer remains intact. With these considerations in mind, polymer materials that can be spin-coated may prove to be good choices in some wavelength ranges. However, most polymers have a backbone comprised of C—H bonds and might contain N—H and O—H bonds which all exhibit characteristic absorption peaks in the 3–3.5 μm wavelength range. Therefore, for our prototype design, in lieu of polymers, we consider inorganic compounds such as alkali halides (e.g., CaF_2) and amorphous alumina (Al_2O_3) as suitable for the spacer layer.

4. Conclusions

In summary, we have demonstrated a novel design that integrates PbTe detectors with ChG waveguides for on chip mid-IR detection. Our simulations show that the use of a spacer layer leads

to a well distributed field along the width of the detector, and that the quantum efficiency of the detector increases as the detector becomes wider. We see that thicker films lead to higher quantum efficiency up to a point but eventually changes in the effective index reduce the quantum efficiency. We have also derived a FoM for the SNR of our evanescently coupled detectors and after factoring in the non-uniformity of the field, shown that narrower detectors yield a higher FoM. We believe that such an integrated sensor design will enable the creation and deployment of low-cost remote sensor arrays with small footprints.

Acknowledgments

Funding for this work has been provided by the US Department of Energy [Contract # DE-NA000421]. This paper has been prepared as an account of work partially supported by an agency of the United States Government. Neither the United States Government nor any agency thereof, nor any of their employees, makes any warranty, express or implied, or assumes any legal liability or responsibility for the accuracy, completeness or usefulness of any information, apparatus, product or process disclosed, or represents that its use would not infringe privately owned rights. Reference herein to any specific commercial product, process, or service by trade name, trademark, manufacturer, or otherwise does not necessarily constitute or imply its endorsement, recommendation, or favoring by the United States Government or any agency thereof. The views and opinions of authors expressed herein do not necessarily state or reflect those of the United States Government or any agency thereof.

References

[1] C. Charlton, M. Giovannini, J. Faist, B. Mizaikoff, Fabrication and characterization of molecular beam epitaxy grown thin-film gaas waveguides for mid-infrared evanescent field chemical sensing, Analytical Chemistry 78 (2006) 4224–4227.
[2] X. Wang, S. Kim, R. Roβbach, M. Jetter, P. Michler, B. Mizaikoff, Ultra-sensitive mid-infrared evanescent field sensors combining thin-film strip waveguides with quantum cascade lasers, Analyst 137 (2012) 2322–2327.
[3] T. Lewi, A. Katzir, Silver halide single-mode strip waveguides for the mid-infrared, Optics Letters 37 (2012) 2733–2735.
[4] K. Richardson, L. Petit, N. Carlie, B. Zdyrko, I. Luzinov, J. Hu, A. Agarwal, L.C. Kimerling, T. Anderson, M. Richardson, Progress on the fabrication of on-chip, integrated chalcogenide glass (ChG)-based sensors, Journal of Nonlinear Optical Physics and Materials 19 (2010) 75–99.
[5] B.J. Eggleton, B.L. -Davies, K. Richardson, Chalcogenide photonics, Nature Photonics 5 (2011) 141–148.
[6] J. Hu, V. Tarasov, N. Carlie, N. Feng, L. Petit, A. Agarwal, K. Richardson, L.C. Kimerling, Si-CMOS-compatible lift-off fabrication of low-loss planar chalcogenide waveguides, Optics Express 15 (2007) 11798–11807.
[7] A. Rogalski, Infrared detectors: an overview, Infrared Physics and Technology 43 (2002) 187–210.
[8] M. Böberl, T. Fromherz, J. Roither, G. Pillwein, G. Springholz, W. Heiss, Room temperature operation of epitaxial lead-telluride detectors monolithically integrated on midinfrared filters, Applied Physics Letters 88 (2006) 041105.
[9] D.E. Bode, Lead salt detectors, in: G. Haas, R.E. Thun (Eds.), Physics of Thin Films, vol. 3, Academic Press, New York, 1966.
[10] J. Wang, J. Hu, X. Sun, A. Agarwal, D. Lim, R. Synowicki, L.C. Kimerling, Structural, electrical and optical properties of thermally evaporated nanocrystalline PbTe films, Journal of Applied Physiology 104 (2008) 053707.
[11] J. Wang, T. Zens, J. Hu, P. Becla, L.C. Kimerling, M.A. Anuradha, Monolithically integrated, resonant-cavity-enhanced dual-band mid-infrared photodetector on silicon, Applied Physics Letters 100 (2012) 211106.
[12] A. Gassenq, N. Hattasan, L. Cerutti, J.B. Rodriguez, E. Tournié, G. Roelkens, Study of evanescently-coupled and grating-coupled GaInAsSb photodiodes integrated on a silicon photonic chip, Optics Express 20 (2012) 11665–11672.
[13] D. Ahn, C. Hong, J. Liu, W. Giziewicz, M. Beals, L.C. Kimerling, J. Michel, J. Chen, F.X. Kärtner, High performance, waveguide integrated Ge photodetectors, Optics Express 15 (2007) 3916–3921.
[14] J. Wang, J. Hu, P. Becla, A.M. Agarwal, L.C. Kimerling, Room-temperature oxygen sensitization in highly textured, nanocrystalline PbTe films: a mechanistic study, Journal of Applied Physics 110 (2011) 083719.
[15] J. Wang, Resonant-cavity-enhanced multispectral infrared photodetectors for monolithic integration on silicon, Ph.D. dissertation, Dept. of Mat. Sci. & Eng., Massachusetts Institute of Technology, Cambridge, MA, 2010.
[16] J.N. Humphrey, R.L. Petritz, Photoconductivity of lead selenide: theory of the mechanism of sensitization, Physical Review 105 (1957) 1736–1740.
[17] R.F. Egerton, C. Juhasz, The effect of oxygen on epitaxial PbTe, PbSe and PbS films, Thin Solid Films 4 (1969) 239–253.
[18] K.S. Bhat, V.D. Das, Electrical-conductivity changes in PbTe and PbSe films on exposure to the atmosphere, Physical Review B 32 (1985) 6713–6719.
[19] D.E. Bode, H. Levinstein, Effect of oxygen on the electrical properties of lead telluride films, Physical Review 96 (1954) 259–265.
[20] D.E. Bode, T.H. Johnson, B.N. McLean, Lead selenide detectors for intermediate temperature operation, Applied Optics 4 (1965) 327–331.
[21] A. Munoz, J. Melendez, M.C. Torquemada, M.T. Rodrigo, J. Cebrian, A.J. de Castro, J. Meneses, M. Ugarte, F. Lopez, G. Vergara, J.L. Hernandez, J.M. Martin, L. Adell, M.T. Montojo, PbSe photodetector arrays for IR sensors, Thin Solid Films 317 (1998) 425–428.
[22] V. Ambegaokar, B.I. Halperin, J.S. Langer, Hopping conductivity in disordered systems, Physical Review B 4 (1971) 2612–2620.
[23] R.L. Petritz, Theory of photoconductivity in semiconductor films, Physical Review 104 (1956) 1508–1516.
[24] J.C. Slater, Barrier theory of the photoconductivity of lead sulfide, Physical Review 103 (1956) 1631–1644.
[25] E.L. Dereniak, G.D. Boreman, Infrared Detectors and Systems, Wiley Interscience, New York, NY USA, 1996.

Biographies

Vivek Singh received Bachelor of Science degrees in physics and materials science from Adelphi University and Columbia University, respectively in 2009. In the same year, he joined the Massachusetts Institute of Technology as a PhD-track graduate student in the Department of Materials Science and Engineering. His current research focuses on developing chalcogenide glass materials and microphotonic devices for mid-infrared applications.

Timothy Zens received his PhD in Materials Science and Engineering and from the Massachusetts Institute of Technology in 2011, investigating *Resonant Cavity Enhanced Detection in Lead Salts*. In 2011, he became an Assistant Professor of Materials Science, Department of Engineering Physics at the Air Force Institute of Technology. In 2012, he became the academic advisor for the Materials Science program at the Air Force Institute of Technology, where he has continued his research activities in long wavelength IR detectors from polycrystalline $Pb_{1-x}Sn_xTe$ films; synthesis of bulk ThO_2 and UO_2 crystals using hydrothermal growth techniques; growth of 2D BN on graphene using molecular beam epitaxy for high power electronics; and orientation patterned infrared non-linear optical materials for infrared countermeasures and terahertz generation.

Juejun Hu received his PhD from MIT in 2009 and is currently an assistant professor in the Department of Materials Science & Engineering at the University of Delaware. His primary research interest focuses on the enhanced photon–matter interactions in nanophotonic structures, with an emphasis on on-chip spectroscopy and chemical sensing applications using novel infrared glasses. His research also covers materials and devices for magneto-optics, photovoltaics, opto-mechanics, and solid state light emitters. He has authored and co-authored over 30 refereed journal publications since 2006 and has been awarded 6 U.S. patents.

Jianfei Wang received the PhD degree in Materials Science and Engineering at Massachusetts Institute of Technology in 2010 on electronic, photonic, and magnetic materials. His research was on resonant-cavity-enhanced multispectral infrared photodetectors for monolithic integration on silicon. Additionally, he was involved in research activities in electrical and magnetic properties of NiO-based materials at Tsinghua University, where he received the Master of Engineering degree in 2005. He is currently a senior design engineer at Sensitron Semiconductor in Deer Park, NY in USA.

Dr. Musgraves conducts research on a variety of challenges in chalcogenide and tellurite glasses. Current research projects include the development of glasses for use in thin-film sensor devices, in fiber-optic infrared light transmission, and in the precision glass molding of optical elements. Additionally, he conducts research into the evolution of glass network structure across multiple length scales, and the impact of this evolution on the resultant properties of the glass. His research in these areas combines efforts in statistics, quantum computational modeling, spectroscopic and thermal analysis in an effort to explore fundamental problems in glass science.

Kathleen Richardson received her PhD in Glass Science and Engineering and from the NYS College of Ceramics at Alfred University in 1992, investigating *Defects in Low-Tg Chalcogenide Glasses*. Following 7 years at the Laboratory for Laser Energetics at the University of Rochester, she went on to become an assistant professor at CREOL and the Department of Chemistry and MMAE at the University of Central Florida (UCF). In 2005, she became Director of the School of Materials Science and Engineering at Clemson University, where she continued her research activities in the area of novel optical glass and glass ceramic materials for the infrared (IR). In 2012, she returned to UCF as a Professor of Optics where she and her group carry out design and fabrication of novel infrared optical materials. She is

a Fellow of SPIE, OSA, the Society of Glass Technology and the American Ceramic Society.

Lionel C. Kimerling is the Thomas Lord Professor of Materials Science and Engineering at MIT and the Director of the MIT Microphotonics Center. Prior to joining MIT, he was the head of the Materials Physics Research Department at AT&T Bell Laboratories. He earned an S.B. in Metallurgical Engineering and a PhD in Materials Science at MIT. He had a fundamental impact on the understanding of the chemical and electrical properties of defects in semiconductors and has pioneered the field of silicon microphotonics. He has been the recipient of several awards and honors and has published more than 300 research articles.

Dr. Anu Agarwal is a Principal Research Scientist at MIT's Microphotonics Center. Her current work centers on the mid-IR (MIR) regime. Although previous silicon microphotonic devices predominantly utilized the NIR range, the MIR regime is extremely interesting for hyperspectral imaging and chem-bio sensing because most chemical and biological toxins have their fingerprints in this range. Her work on MIR materials and devices is creating a planar, integrated, Si-CMOS-compatible microphotonics platform which will enable on-chip imaging and sensing applications. Prior to coming to MIT she received her doctoral degree in Electrical Engineering from Boston University, where she investigated the spatial extent of point defect interactions in silicon.